

# Effect of using MgO coating with multiple coatings on the optical properties of a five-layer stack

Zainab I. Al-Assadi  

Physics Department, College of Science, Mustansiriyah University, Baghdad, Iraq.

Received 25/09/2023, Revised 12/02/2024, Accepted 14/02/2024, Published Online First 20/02/2024,  
Published 01/09/2024



© 2022 The Author(s). Published by College of Science for Women, University of Baghdad.

This is an open-access article distributed under the terms of the [Creative Commons Attribution 4.0 International License](https://creativecommons.org/licenses/by/4.0/), which permits unrestricted use, distribution, and reproduction in any medium, provided the original work is properly cited.

## Abstract

A high refractive index (H) 1.7376 dielectric material MgO was used, and four separate low refractive index (L) dielectric materials, BaF<sub>2</sub> (Barium fluoride, 1.4825), Al<sub>2</sub>O<sub>3</sub> (Alumina, 1.5322), GdF<sub>3</sub> (Gadolinium Fluoride, 1.59) and LaF<sub>3</sub> (Lanthanum Fluoride, 1.6056) were added as optical coatings. Five layers across two designs were used for each option. The first format was Glass/H/L/H/L/H, while the second was Glass/L/H/L/H/L. These were tested using MATLAB to calculate the optical properties ( $M$ ,  $R_{vis}$ ,  $R_{sol}$ , and  $T_{sol}$ ) of the resulting optical coatings were calculated to determine which coating the most efficient for colouring the glass of solar systems used as building façades. The results explained, using the first design, just two coatings were efficient with respect to colouration, with MgO+BaF<sub>2</sub> being the most efficient with values of  $M=8.25$  and  $R_{vis}=38.2$ . The MgO+Al<sub>2</sub>O<sub>3</sub> coating was the next most efficient, with values of  $M=6.12$  and  $R_{vis}=31.24$ , the required values for the merit factor ( $M$ ) and  $R_{vis}$  which make the coating efficient for colouration are 6% and 12%, respectively. Further, in this case, only one sharp and regular reflection peak of colouration in the visible region was observed. In the first design the refractive index was found to be inversely proportional to the optical properties of the coating, and thus to the colour efficiency of the coating: the MgO+BaF<sub>2</sub> coating was thus deemed more efficient than the MgO+Al<sub>2</sub>O<sub>3</sub> coating. The second design was considered inefficient for colouration for all four coatings, as none of these met the required values for ( $M$ ) and  $R_{vis}$ .

**Keywords:** Coloured glazing, Facade integration solar systems, Multi-layer coating, Optical interference filter, Thin films.

## Introduction

Over 40% of the world's energy is used by high-rise buildings and smart cities, a trend that is expected to continue in the near future as a result of growing populations, long-term building utilisation, and a growing need for higher building comfort levels. Buildings are thus closely linked to CO<sub>2</sub> production and thus contribute significantly to climate change and global warming, resulting in ocean acidity and rising sea levels as a result of ice cap melting, which is an issue, as the worldwide community has set a goal of achieving net-zero carbon emissions by 2050

in order to limit global temperature rises to 1.5 °C<sup>1</sup>. Previous studies on façade integration have primarily focused on energy considerations; however, to maximize power productivity, façade integrated photovoltaic (FIPVs) are required as part of the full architectural design rather than being only secondary considerations. Typically, building roofs are now coated with opaque photovoltaic products, however, and conventional opaque photovoltaics' glossy surfaces, dark-blue or black colouring, and inflexible geometries make them challenging to integrate as

cladding or shading systems in many building façades. As PV technology has advanced, new products to overcome these obstacles have begun to appear,<sup>2,3</sup> however, and the development of coloured solar panels that offer low costs and high conversion efficiency is likely to be crucial for the widespread market penetration of building-integrated photovoltaic (BIPV). Solar energy harvesting via photovoltaics is among the most promising technologies for the development of self-sustainable constructed environments: architects, construction companies, and homeowners should thus prioritise architectural freedom and aesthetics when implementing solar panels in buildings. Solar panels directly incorporated into a building's façade, or BIPV, are therefore a crucial tool, offering architects the ability to use nearly every portion of a building's surface to generate energy without compromising aesthetics<sup>4</sup>.

Due to shortages of conventional energy and concerns about increases in pollutants, interest in renewable energy, particularly solar energy, has increased in recent years. Solar energy offers opportunities for greater sustainability in terms of power while also creating new jobs in the sector<sup>5,6</sup>, and among the various typologies, of renewable technologies, solar-based options offer the greatest promise in terms of energy production and decreases in carbon emissions due to the large amount of solar radiation potentially available. Photovoltaic (PV) panels, Solar Thermal Collectors (STC), and hybrid systems are thus among the most commonly used building technologies<sup>7</sup>, and building-integrated solar energy systems using photovoltaics, solar thermal, or various combinations of the two, could readily supply most new buildings with power and/or heat<sup>8</sup>.

However, architects demand aesthetic flexibility when selecting such systems for their designs. People's perceptions of the urban context and the creation of impressions of cities are greatly influenced by the colours of the façade,<sup>9</sup> for example, and traditional commercial photovoltaics' dark blue and black colours do not fit with the colours of most city façades: a black facade is often acceptable in a solitary case, especially in city centres, but it is not often seen as appropriate for widespread usage. Kromatix TM technology offers one solution to this, using multilayered interference filters to give solar panels products variable colours by utilising view angles<sup>10</sup>. Other viable approaches include the use of coloured anti-reflective coatings

on solar cells<sup>11</sup>, yet colour tastes are typically incongruent from the architectural and energy perspectives<sup>12</sup>. Many real-world projects utilise pixelization designs within their architectural language to generate the architects' desired façade images in terms of seamless colour transitions, meticulously organizing the façade parts across various different colours, for example.

People's opinion of beauty is greatly influenced by colour, and the guidelines or principles regarding the best colour pairings for heightened aesthetic perception have been studied for millennia. Science and art have thus both been involved in the development of photovoltaic systems commonly installed on roof areas in the past. However, due to limited roof space, there is now a growing desire for photovoltaics to be installed on building facade<sup>13</sup>. FIPV is a novel and significant method of utilizing solar energy in the built environment, yet few architectural studies have been conducted on FIPV, particularly with respect to colour performance. The growing need for nearly zero-energy buildings can be significantly supported by BIPV, however, as such systems offer promising results for harvesting the plentiful available renewable solar energy in the constructed environment<sup>14</sup>. Real world case studies have demonstrated that BIPV can offer an appealing and sustainable alternative for building façade renovation projects<sup>15</sup>. However, from the perspective of urban planners and architects, their dark colour is the biggest barrier to the use of solar panels for building facades. A global investigation of overcoming the hurdles preventing wider solar thermal and solar panels system use thus dwelt on the idea of maximising colour harmony<sup>9</sup>.

In this research, a multi-layer method was used, combining a high refractive index (H) 1.7376 dielectric material (MgO) with four low refractive index (L) dielectric materials, BaF<sub>2</sub> (Barium fluoride, 1.4825), Al<sub>2</sub>O<sub>3</sub> (Alumina, 1.5322), GdF<sub>3</sub> (Gadolinium Fluoride, 1.59) and LaF<sub>3</sub> (Lanthanum Fluoride, 1.6056), to form optical coatings across five layers in two designs. The first layer design was Glass/H/L/H/L/H, while the second was Glass/L/H/L/H/L. These were tested using MATLAB, with the optical properties (M, R<sub>vis</sub>, R<sub>sol.</sub>, and T<sub>sol.</sub>) of the four optical coatings thus calculated, to determine which coating offers the most efficient way to colour the glass for solar systems, and, similarly, which might be deemed excessively inefficient.

## Theoretical Part

The simplest antireflection coating model involves using a single-layered substrate: the amount of antireflection is then determined by how much light is cancelled by the coating's upper and lower surfaces. The reflection intensity from both surfaces must therefore be equal to completely eliminate reflection. The ratio of the refractive indices of air ( $n_0$ ) and coating ( $n_1$ ) thus ought to match the ratio between  $n_1$  and the substrate's refractive index ( $n_u$ )<sup>16</sup>:

$$\frac{n_0}{n_1} = \frac{n_1}{n_u} \dots \dots \dots 1$$

At a design wavelength ( $\lambda$ ), the physical film thickness ( $t_j$ ) would thus be<sup>17</sup>

$$n_1 \cdot t_j = \frac{\lambda}{4} \dots \dots \dots 2$$

One minimum is provided by this type of antireflection coating in the reflection profile; however, additional layers are needed for multiple minima, which are required by the underlying theory of the optical matrix method for developing mathematical models for two-, three-, or multi-layer antireflection coatings. A layer or multi-layer (stack of thin films) of the chosen material with a thickness ranging from one nanometer to several micrometers is known as a thin film<sup>16,17</sup>.

Eq. 3 offers the fundamental statement for the construction of an n-layer structure, offering a mathematical paradigm for the design of multilayer antireflection coatings<sup>17</sup>:

$$\begin{bmatrix} B \\ D \end{bmatrix} = \sum_{j=1}^N \begin{bmatrix} \cos \delta_j & \left(\frac{i}{n_j}\right) \sin \delta_j \\ i \cdot n_j \cdot \sin \delta_j & \cos \delta_j \end{bmatrix} \begin{bmatrix} 1 \\ n_u \end{bmatrix} \dots \dots 3$$

$\begin{bmatrix} B \\ D \end{bmatrix}$  indicates the sum of the amplitudes of light propagation's electrical and magnetic fields. The refractive index of the substrate is  $u$ , while the  $j$ th layer's refractive index is  $j$ , where  $j$  is 1, 2, 3, .... The value of  $j$  represents the layer's phase thickness at each wavelength, equivalent to<sup>18</sup>

$$\delta_j = \frac{2\pi}{\lambda} n_j t_j \dots \dots \dots 4$$

Optical admittance ( $Y$ ) is defined as the ratio of  $D$  to  $B$ <sup>17</sup>:

$$Y = \frac{D}{B} \dots \dots 5$$

The matrix of the characteristics for  $n$  different coatings at the design wavelength ( $\lambda$ ) is represented in Eq. 6. This can be used to compute the combined reflectance for multiple thin coatings<sup>18</sup>:

$$L = L_1 \cdot L_2 \cdot L_3 \dots \dots \dots L_n \dots \dots 6$$

Each thin film layer is represented by the following 2x2 matrix<sup>17</sup>:

$$L_j = \begin{bmatrix} \cos \delta_j & \left(\frac{i}{n_j}\right) \sin \delta_j \\ i \cdot n_j \cdot \sin \delta_j & \cos \delta_j \end{bmatrix} \dots \dots 7$$

Eqs. 8 and 9 can then be used to calculate the coefficient of reflection ( $r$ ) as well as the reflectance ( $R$ ).<sup>17,18</sup>

For  $N$ -layer designs of antireflection coatings, the optical matrix technique can be used. The primary concept behind this technology is to match the incidental light's  $E$  and  $H$  fields at the interfaces of multilayer optical coatings.

The optical interference matrix offers an efficient method for calculating film reflectivity<sup>19</sup>.

$$r = \frac{n_0 - Y}{n_0 + Y} \dots \dots 8$$

$$R = rr = \begin{bmatrix} n_0 - Y \\ n_0 + Y \end{bmatrix} \begin{bmatrix} n_0 - Y \\ n_0 + Y \end{bmatrix} \dots \dots \dots 9$$

The reflectance matrix equation for a quarter wave thickness at normal incidence is thus<sup>17-20</sup>

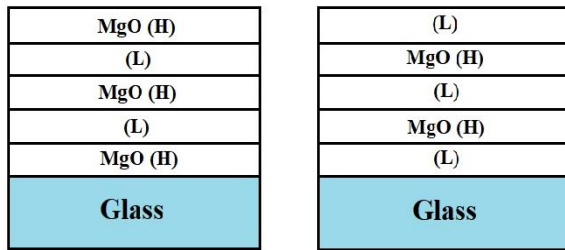
$$\begin{bmatrix} 0 & in_j^{-1} \\ in_j & 0 \end{bmatrix} \dots \dots \dots 10$$

where  $n$  is the layer's refractive index, in which  $j=1, 2, 3, \dots$

Morphological differences in films may cause the optical reflection to change, however<sup>21</sup>.

## Materials and Methods

In this research, a high refractive index (H) 1.7376 dielectric material MgO was used alongside four low refractive index (L) dielectric materials, BaF<sub>2</sub> (Barium fluoride, 1.4825), Al<sub>2</sub>O<sub>3</sub> (Alumina, 1.5322), GdF<sub>3</sub> (Gadolinium Fluoride, 1.59) and LaF<sub>3</sub> (Lanthanum Fluoride, 1.6056) to form optical coatings across five layers in two designs on a glass substrate. The first design was thus Glass/H/L/H/L/H, while the second was Glass/L/H/L/H/L for quarter wave thicknesses, as shown in Fig. 1. This was designed in MATLAB.



(a) Glass/H/L/H/L/H

(b) Glass/L/H/L/H/L

**Figure 1. Two multilayer optical designs: Glass/H/L/H/L/H and Glass/L/H/L/H/L.**

## Results and Discussion

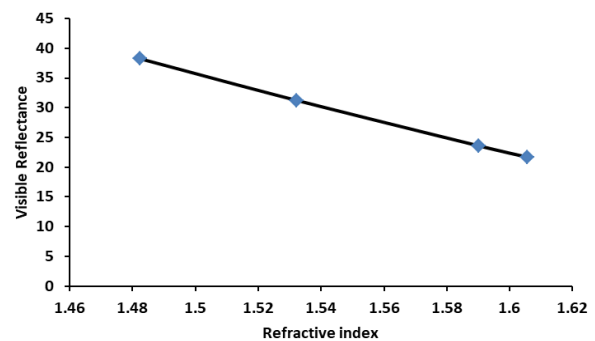
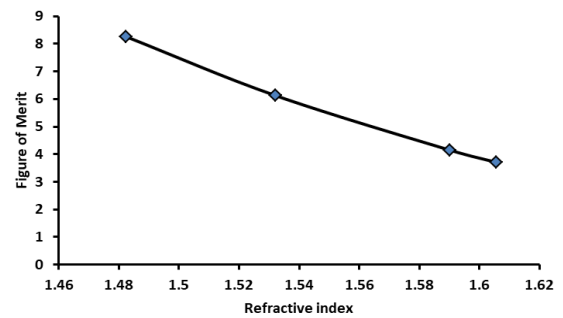
The optical properties of the four optical coatings were calculated as shown in Table 1.

**Table 1. The optical properties for four optical coatings constructed from five layers using the G/H/L/H/L/H/Air design.**

Layers of	$n_L$	Meri	$R_{vis}$	$R_{sol}$	$T_{sol}$
MgO+	1.482	8.255	38.23	4.631	95.36
BaF <sub>2</sub>	5	7	26		9
MgO+Al <sub>2</sub>	1.532	6.122	31.24	5.102	94.89
O <sub>3</sub>	2	3	61	8	72
MgO+	1.59	4.153	23.61	5.686	94.31
GdF <sub>3</sub>	2	83	7	33	
MgO+	1.605	3.708	21.69	5.849	94.15
LaF <sub>3</sub>	6	0	16	9	01

The results show that, in the first case (Glass/H/L/H/L/H), the values of M,  $R_{vis}$ ,  $T_{sol}$  increase as the values of the refractive indices decrease, while the  $R_{sol}$  values increase with any increase in the refractive indices. This represents the amount of loss in the system, as shown in Fig. 2.

The optical properties, most specifically the Figure of Merit (M), Visible Reflectance ( $R_{vis}$ ), Solar Reflectance ( $R_{sol}$ ), and Solar Transmittance ( $T_{sol}$ ), of the four resulting optical coatings for each design were calculated to determine which coating might be the most efficient to colour the glass for solar systems, and which coatings would be inefficient.



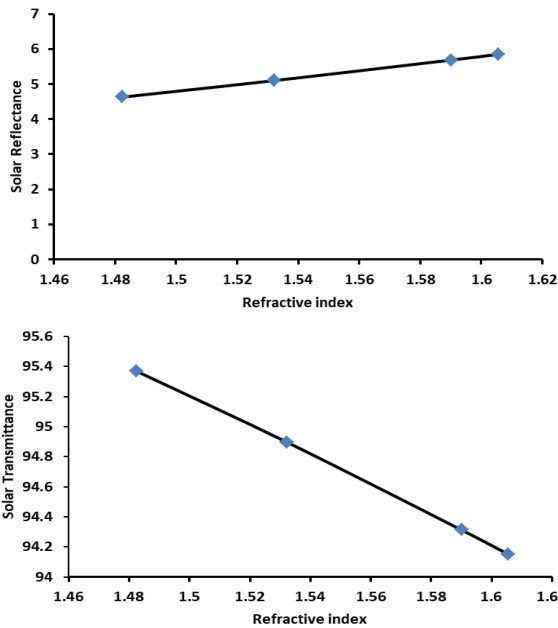


**Figure 2. Variation in optical properties (Figure of merit (M),  $R_{vis}$ ,  $T_{sol}$ , and  $R_{sol}$ ) for multilayer optical coatings by refractive index.**

The results show that the coating using  $MgO+BaF_2$  is the most efficient for colouring purposes, with values of  $M=8.25$  and  $R_{vis}=38.2$ ; the next most efficient is the coating with  $MgO+Al_2O_3$ , which demonstrated values of  $M=6.12$  and  $R_{vis}=31.24$ , respectively. The required values of  $M$  and  $R_{vis}$  that allow a coating to be seemed efficient for colouring purposes are 6% and 12%, respectively, as explained

**Table 2. Optical properties for four optical coatings across five layers using the G/L/H/L/H/L/Air design.**

Layers of	$n_L$	Merit	$R_{vis}$	$R_{sol}$	$T_{sol}$
$MgO+BaF_2$	1.4825	1.7186	8.028	4.6713	95.3287
$MgO+Al_2O_3$	1.5322	1.275	6.5677	5.1512	94.8488
$MgO+GdF_3$	1.59	1.0302	5.9066	5.7336	94.2664
$MgO+LaF_3$	1.6056	1.0108	5.8996	5.8366	94.1634

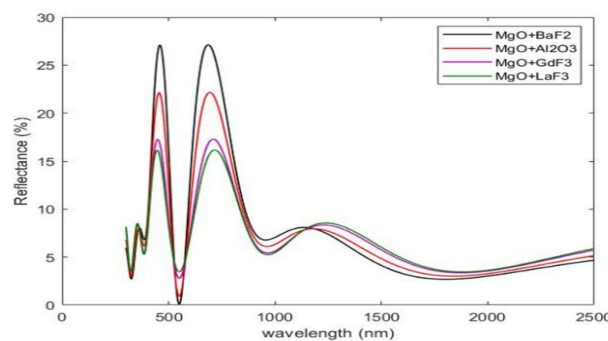


**Figure 4. Irregular behaviours of the reflection peak in the visible region for the four coatings using the second optical design (Glass/L/H/L/H/L).**

in reference <sup>22</sup>. The remainder of the coatings must thus be considered inefficient, as they do not achieve the required values of  $M$  and  $R_{vis}$ , Fig. 3 illustrates the behaviour of the reflection peak for all four coatings, showing that there is one regular reflection peak in the visible region for these four coatings, but that the reflection peak of the  $MgO+BaF_2$  coating is the best at 45%.

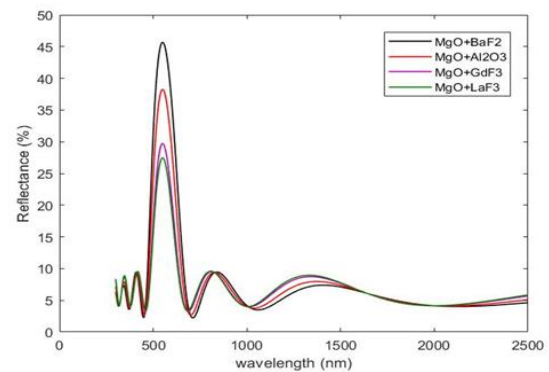


**Figure 3. Behaviour of the reflection peak in the visible region for four coatings using the first optical design (Glass/H/L/H/L/H).**

In the second case, when the design used is Glass/L/H/L/H/L, all the coatings must be considered inefficient for colouring, as they do not reach the required values of  $M$  and  $R_{vis}$ , as shown in Table 2. Further, the reflection peak for all coatings is irregular, with no singular sharp peak in the visible region representing peak colouration, as shown in Fig. 4.

## Conclusion

Using the first design (Glass/H/L/H/L/H) for five layers, just two coatings are shown to be efficient in terms of the necessary colouration ( $\text{MgO}+\text{BaF}_2$  and  $\text{MgO}+\text{Al}_2\text{O}_3$ ), based on them achieving the required values for the figure of merit (M) and  $R_{\text{vis}}$ , as well as showing only a singular sharp regular reflection peak of colouration in the visible region. The refractive index in the first design is inversely proportional to the optical properties of the coating, and hence the colour efficiency of the coating, however, leading to

the  $\text{MgO}+\text{BaF}_2$  coating being more efficient than the  $\text{MgO}+\text{Al}_2\text{O}_3$  coating in terms of colouration. The second design (Glass/L/H/L/H/L) for five layers must be considered inefficient for colouration for all four coating types ( $\text{MgO}+\text{BaF}_2$ ,  $\text{MgO}+\text{Al}_2\text{O}_3$ ,  $\text{MgO}+\text{GdF}_3$ , and  $\text{MgO}+\text{LaF}_3$ ), however, as the required values for the figure of merit (M) and  $R_{\text{vis}}$  are not achieved in any case, and all coatings show irregular reflection peaks in the visible region.

## Acknowledgment

This study was supported by Mustansiriyah University ([www.uomustansiriyah.edu.iq](http://www.uomustansiriyah.edu.iq)), Baghdad, Iraq.

## Authors' Declaration

- Conflicts of Interest: None.
- I hereby confirm that all the Figures and Tables in the manuscript are mine. Furthermore, any Figures and images, that are not mine, have been

- included with the necessary permission for re-publication, which is attached to the manuscript.
- Ethical Clearance: The project was approved by the local ethical committee at Mustansiriyah University.

## References

1. Basher MK, Nur-E-Alam M, Rahman MM, Hinckley S, Alameh K. Design, development, and characterization of highly efficient colored photovoltaic module for sustainable buildings applications. *Sustainability*. 2022; 14(7): 4278. <https://doi.org/10.3390/su14074278>
2. Xiang C, Matusiak BS, editors. *Facade Integrated Photovoltaic, state of the art of Experimental Methodology*. IOP Conf Ser Earth Environ Sci. 2019; 352: 012062; IOP Publishing; <https://doi.org/10.1088/1755-1315/352/1/012062>
3. Costanzo V, Yao R, Essah E, Shao L, Shahrestani M Oliveira A. A method of strategic evaluation of energy performance of Building Integrated Photovoltaic in the urban context. *J Clean Prod*. 2018; 184: 82-91; <https://doi.org/10.1016/j.jclepro.2018.02.139>
4. Habets R, Vroon Z, Erich B, Meulendijks N, Mann D, Buskens P, editors. *Structural color coatings for high performance BIPV*. Conf. Ser. Earth Environ. Sci. 2021; 855: 1-5; IOP Publishing; <https://doi.org/10.1088/1755-1315/855/1/012011>
5. Mahdi HA, AL-Joboory HNS, Abdula AG, Hameed AA, Rasheed AK. Design and Performance Investigation of a Solar-Powered Biological Greywater Treatment System in the Iraqi Climate. *Baghdad Sci J*. 2022; 19(3): 0670; <https://doi.org/10.21123/bsj.2022.19.3.0670>
6. Mahmood YH, Majeed MA. Design of a Simple Dust Removal System for a Solar Street Light System. *Baghdad Sci J*. 2022; 19(5): 1123. <https://doi.org/10.21123/bsj.2022.6467>
7. Agathokleous R, Barone G, Buonomano A, Forzano C, Kalogirou SA Palombo A. Building façade integrated solar thermal collectors for air heating: experimentation, modelling and applications. *Appl Energy*. 2019; 239: 658-679. <https://doi.org/10.1016/j.apenergy.2019.01.020>
8. Eder G, Peharz G, Trattnig R, Bonomo P, Saretta E, Frontini F, et al. Coloured bipv: Market, research and development. IEA Photovoltaic Power Systems Programme. Report IEA-PVPS T15-07. 2019.
9. Xiang C, Matusiak BS, Røyset A, Kolås T. Pixelization approach for façade integrated coloured photovoltaics-with architectural proposals in city context of Trondheim, Norway. *J Sol. Energy*. 2021; 224: 1222-1246; <https://doi.org/10.1016/j.solener.2021.06.079>
10. Jolissaint N, Hanbali R, Hadorn J-C, Schüler A. Colored solar façades for buildings. *Energy Procedia*. 2017; 122: 175-180. <https://doi.org/10.1016/j.egypro.2017.07.340>

11. Meng L, Zhang Y, Wan X, Li C, Zhang X, Wang Y, et al. Organic and solution-processed tandem solar cells with 17.3% efficiency. *Science*. 2018; 361(6407): 1094-1098; <https://doi.org/10.1126/science.aat2612>
12. Røyset A, Kolås T, Jelle BP. Coloured building integrated photovoltaics: Influence on energy efficiency. *Energy Build.* 2020; 208: 109623; <https://doi.org/10.1016/j.enbuild.2019.109623>
13. Chen T, Lau S, Zhang J, Xue X, Lau S, Khoo Y. A design-driven approach to integrate high-performance photovoltaics devices on the building façade. *IOP Conf Ser Earth Environ Sci.* 2019; 294: 1-7. IOP Publishing: 012030; <https://doi.org/10.1088/1755-1315/294/1/012030>
14. Debbarma M, Pala NA, Kumar M, Bussmann RW. Traditional knowledge of medicinal plants in tribes of Tripura in northeast, India. *Afr J Tradit Complement Altern Med* 2017; 14(4): 156-168. <https://doi.org/10.21010/ajtcam.v14i4.19>
15. Saretta E, Caputo P, Frontini F. A review study about energy renovation of building facades with BIPV in urban environment. *Sustain. Cities Soc.* 2019; 44: 343-355; <https://doi.org/10.1016/j.scs.2018.10.002>
16. Afkhami Z, Iezzi B, Hoelzle D, Shtein M, Barton K. Electrohydrodynamic Jet Printing of One-Dimensional Photonic Crystals: Part I—An Empirical Model for Multi-Material Multi-Layer Fabrication. *Adv Mater Technol.* 2020; 5(10): 2000386; <https://doi.org/10.1002/admt.202000386>
17. Macleod HA. Thin-film optical filters. CRC press. 5th Edition 2017; 696P, Boca Raton. <https://doi.org/10.1201/b21960>
18. Mansoor M, Zaman S, Ali L, Khan S. Design of three-layer antireflection coating for high reflection index lead chalcogenide. *Mater Res.* 2019; 22. <https://doi.org/10.1590/1980-5373-MR-2018-0534>
19. Keskar D, Survase S, Thakurdesai M. Reflectivity simulation by using transfer matrix method. *J Phys Conf Ser.* 2021; 012051. <https://doi.org/10.1088/1742-6596/1913/1/012051>
20. Garlisi C, Trepci E, Li X, Al Sakkaf R, Al-Ali K, Nogueira RP, et al. Multilayer thin film structures for multifunctional glass: Self-cleaning, antireflective and energy-saving properties. *Appl Energy.* 2020; 264: 114697. <https://doi.org/10.1016/j.apenergy.2020.114697>
21. Hameed MM, Al-Samarai A-ME, Aadim KA. Synthesis and characterization of gallium oxide nanoparticles using pulsed laser deposition. *Iraqi J Sci.* 2020; 2582-2589; <https://doi.org/10.24996/ijsc.2020.61.10.14>
22. Schüler A, Roecker C, Boudaden J, Oelhafen P, Scartezzini J-L. Potential of quarterwave interference stacks for colored thermal solar collectors. *Sol Energy.* 2005; 79(2): 122-130. <https://doi.org/10.1016/j.solener.2004.12.008>

## تأثير استخدام طلاء MgO مع طلاءات متعددة على الخصائص البصرية لزرمة مكونة من (5) طبقات

زينب ارحيم حسين الاسدي

قسم الفيزياء، كلية العلوم، الجامعة المستنصرية، بغداد، العراق.

### الخلاصة

تم استخدام المادة العازلة MgO ذات معامل الانكسار العالي (H) 1.737 مع أربعة مواد عازلة BaF<sub>2</sub> (فلوريد الباريوم) و Al<sub>2</sub>O<sub>3</sub> (الألومينا) و GdF<sub>3</sub> (فلوريد الجادولينيوم) و LaF<sub>3</sub> اللانثانوم فلورايد ذات معامل انكسار واطيء (L) 1.4825 و 1.5322 و 1.59 و 1.6056 على التوالي كطلاءات بصرية لخمس طبقات وللتصميم الأول هو (Glass/H/L/H/L/H) والثاني (Glass/L/H/L/H/L)، باستخدام برنامج MATLAB. تم حساب الخصائص البصرية (M، R<sub>vis</sub>، R<sub>sol</sub>، T<sub>sol</sub>) للطلاءات البصرية الأربعة المكونة، وذلك لمعرفة أي طلاء منها كفوء لتلويين زجاج الأنظمة الشمسية المستخدمة كواجهات للأبنية وأيها غير كفوء. تظهر النتائج أنه في التصميم الأول (Glass/H/L/H/L/H) للطبقات الخمس، يوجد طلاءان فقط لهما كفاءة للتلويين، وهما الطلاءان (MgO + BaF<sub>2</sub>) و (MgO + Al<sub>2</sub>O<sub>3</sub>)، لأنهما يحققان القيم المطلوبة من عامل الجدارة (M) والانعكاسية المرئية R<sub>vis</sub> حيث ان القيم المطلوبة لقيم عامل الجدارة (M) و R<sub>vis</sub> والتي تجعل الطلاء كفوءاً للتلويين هي 6% و 12% على التوالي، ولهما قمة انعكاس منتظمة واحدة للتلويين في المنطقة المرئية. في التصميم الأول، يتناسب معامل الانكسار عكسياً مع الخصائص البصرية للطلاء وبالتالي كفاءة تلويين الطلاء، مما يعني أن طلاء (MgO + BaF<sub>2</sub>) أكثر كفاءة من طلاء (MgO + Al<sub>2</sub>O<sub>3</sub>) للتلويين. يعتبر التصميم الثاني (Glass/L/H/L/H/L) للطبقات الخمس غير كفوء للتلويين للطلاءات الأربعة (MgO + BaF<sub>2</sub>)، (MgO + Al<sub>2</sub>O<sub>3</sub>)، (MgO + GdF<sub>3</sub>)، لأنها لا تمتلك القيم المطلوبة من (M) و R<sub>vis</sub>.

**الكلمات المفتاحية:** التزجيج الملون، تكامل واجهات المنظومات الشمسية، طلاء متعدد الطبقات، المرشح البصري التداخلي، الاغشية الرقيقة.